

Stress Waves in a Generalized Thermo Elastic Polygonal Plate of Inner and Outer Cross Sections

R. Selvamani*

Department of Mathematics, Karunya University, Coimbatore-641 114, Tamil Nadu, India

Received 9 February 2017; accepted 30 March 2017

ABSTRACT

The stress wave propagation in a generalized thermoelastic polygonal plate of inner and outer cross sections is studied using the Fourier expansion collocation method. The wave equation of motion based on two-dimensional theory of elasticity is applied under the plane strain assumption of generalized thermoelastic plate of polygonal shape, composed of homogeneous isotropic material. The frequency equations are obtained by satisfying the irregular boundary conditions along the inner and outer surface of the polygonal plate. The computed non-dimensional wave number and wave velocity of triangular, square, pentagonal and hexagonal plates are given by dispersion curves for longitudinal and flexural antisymmetric modes of vibrations. The roots of the frequency equation are obtained by using the secant method, applicable for complex roots.

© 2017 IAU, Arak Branch. All rights reserved.

Keywords : Waves in thermal plate; Piezoelectric plate; Layered plate; Collocation method; Thermal relaxation times; Temperature sensors.

1 INTRODUCTION

THE effect of mechanical and thermal disturbance in an elastic body is known as thermoelasticity. In the classical coupled and uncoupled theory of thermo elasticity, the heat conductions are of diffusion type which will propagate infinite heat pulses and is physically absurd. To overcome such defect, the generalized theories of thermoelasticity of the coupled theory which will propagate finite heat pulses, with temperature-rate dependent have been developed. The propagation of stress waves in thermoelastic materials with polygonal shape has many applications in various fields of science and technology, namely, atomic physics, industrial engineering, thermal power plants, submarine structures, pressure vessels, aerospace, chemical pipes and metallurgy. Nagaya [1,2,3,4,5] devised a method to solve wave propagation in polygonal plates and to find out the phase velocities in different modes of vibrations, namely, longitudinal, torsional and flexural, by constructing frequency equations. He formulated the Fourier expansion collocation method for this purpose and the same method is used in this paper. Lord and Shulman [6] developed the generalized theory of thermo elasticity by involving one relaxation time for isotropic homogeneous media, which is called the first generalization to the coupled theory of elasticity. These equations determine the finite speeds of propagation of heat and displacement distributions. Dhaliwal and Sherief [7] were obtained the corresponding equations for anisotropic materials. A generalization of thermal signals with two relaxation times was proposed by Green and Laws [8]. Green and Lindsay [9] obtained an explicit version of the constitutive equations. These equations were also obtained independently by Suhubi [10]. This theory contains two constants that act as relaxation times and modify not only the heat equations, but also all the equations of the coupled theory. The classical Fourier's law of heat conduction is not violated if the medium under consideration has

*Corresponding author.

E-mail address: selvam1729@gmail.com (R.Selvamani).

a center of symmetry. Erbay and Suhubi [11] studied the longitudinal wave propagation in a generalized thermoplastic infinite cylinder and obtained the dispersion relation for a constant surface temperature of the cylinder. Sharma and Sharma [12] investigated the free vibration of homogeneous transversely isotropic thermoelastic cylindrical panel using Bessel functions. Asymptotic wave motion in transversely isotropic plates was analyzed by Sharma and Kumar [13]. Ashida and Tauchert [14] have presented the temperature and stress analysis of an elastic circular cylinder in contact with heated rigid stamps. Later, Ashida [15] presented the thermally - induced wave propagation in a piezoelectric plate. Tso and Hansen [16] studied the wave propagation through cylinder/plate junctions. Heyliger and Ramirez [17] analyzed the free vibration characteristics of laminated circular piezoelectric plates and disc by using a discrete-layer model of the weak form of the equations of periodic motion. Thermal deflection of an inverse thermoelastic problem in a thin isotropic circular plate was presented by Gaikward and Deshmukh [18]. Varma [19] presented the propagation of waves in layered anisotropic media in generalized thermoelasticity in an arbitrary layered plate. Ponnusamy [20,21] studied the wave propagation in a generalized thermoelastic solid cylinder of arbitrary cross-section and wave propagation in a piezoelectric solid bar of circular cross-section immersed in fluid, respectively using the Fourier expansion collocation method. Jiangong et al., [22] discussed the circumferential thermoelastic waves in orthotropic cylindrical curved plates without energy dissipation. Later, Jiangong with Tonglong [23] presented the propagation of thermoelastic waves in orthotropic spherical curved plates subjected to stress-free, isothermal boundary conditions in the context of the Green–Naghdi (GN) generalized thermoelastic theory (without energy dissipation). Jiangong et al., [24] analyzed the wave propagation of generalized thermoelastic waves in functionally graded plates without energy dissipation. The effect of viscosity on wave propagation in anisotropic thermoelastic medium with Three-phase-lag model has been investigated by Rajneesh Kumar et al.[25]. Later, Rajneesh Kumar and Ibrahim[26] studied the response of thermal source in initially stressed generalized thermoelastic half-space with voids. Recently, Rajneesh Kumar et al[27] evaluated the analytical numerical solution of thermoelastic interactions in a semi-infinite medium with one relaxation time. The dispersion analysis of generalized magneto-thermoelastic waves and the wave propagation in a magneto-thermo elastic waves in a transversely isotropic cylindrical panel using the wave propagation approach were investigated respectively by Ponnusamy and Selvamani [28,29]. The wave propagation in a generalized thermo elastic plate immersed in fluid was analyzed by Selvamani and Ponnusamy [30]. Recently, Selvamani and Ponnusamy [31] have studied the dynamic response of a solid bar of cardioidal cross-sections immersed in an inviscid fluid using Fourier expansion collocation method.

In this paper, free vibration of generalized thermoelastic polygonal plate of inner and outer cross sections composed of homogeneous isotropic material is studied based on Lord-Shulman (LS) thermo elastic equation using the Fourier expansion collocation method along the irregular boundaries. The solutions to the equations of motion for an isotropic medium is obtained by using the two dimensional theory of elasticity. The computed non-dimensional wave number and velocity of triangular, square, pentagonal and hexagonal plates are given by dispersion curves for longitudinal and flexural antisymmetric modes of vibrations.

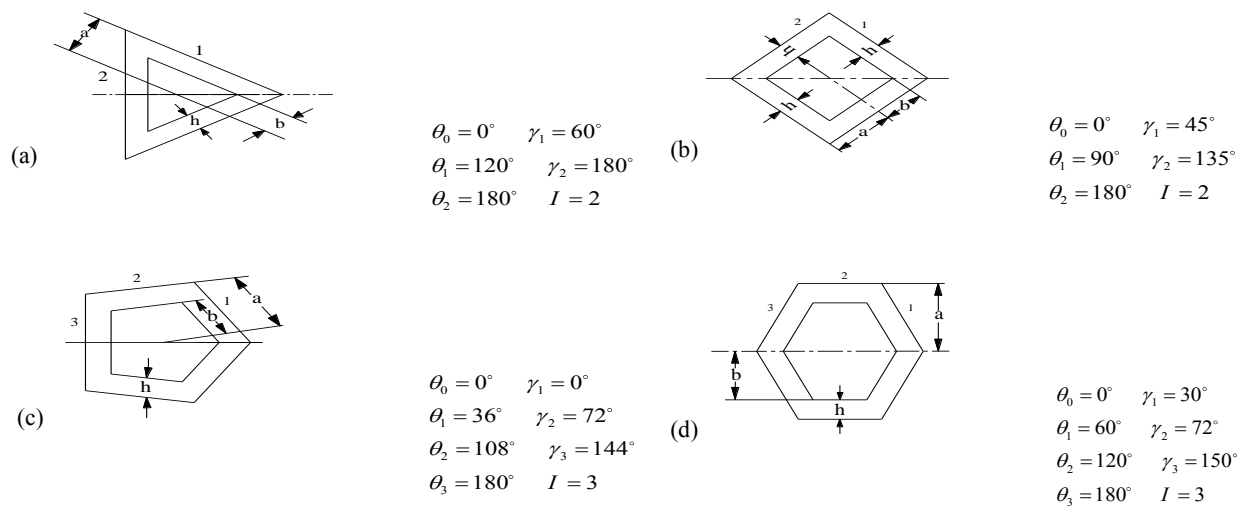


Fig.1 Geometry of ring shaped polygonal plates((a) Triangle (b) Square (c)Pentagon(d) Hexagon).

2 MODEL OF THE PROBLEM

The author considers a homogeneous, isotropic, thermally conducting elastic polygonal plate with uniform temperature T_0 in the undisturbed state initially. The system displacements and stresses are defined by the polar coordinates r and θ in an arbitrary point inside the plate and denote the displacements u_r in the direction of r and u_θ in the tangential direction θ . The in-plane vibration and displacements of polygonal plate is obtained by assuming that there is no vibration and displacement along the z -directions in the cylindrical coordinate system (r, θ, z) . The two dimensional stress equations of motion, strain displacement relations and heat conduction equation in the absence of body forces for a linearly elastic medium are considered from Sharma and Sharma [12] as:

$$\sigma_{r,r} + r^{-1}\sigma_{r\theta,\theta} + r^{-1}(\sigma_{rr} - \sigma_{\theta\theta}) = \rho\ddot{u}_r, \quad \sigma_{r\theta,r} + r^{-1}\sigma_{\theta\theta,\theta} + 2r^{-1}\sigma_{r\theta} = \rho\ddot{u}_\theta \quad (1)$$

$$K(T_{,rr} + r^{-1}T_{,r} + r^{-2}T_{,\theta\theta}) - \rho c_v(\dot{T} + t_0\ddot{T}) = T_0 \left(\frac{\partial}{\partial t} + \delta_{1k}t_0 \frac{\partial^2}{\partial t^2} \right) \left[\beta(u_{r,r} + r^{-1}(u_{\theta,\theta} + u_r)) \right] \quad (2)$$

and

$$\sigma_{rr} = \lambda(e_{rr} + e_{\theta\theta}) + 2\mu e_{rr} - \beta(T + t_1\delta_{2k}\dot{T}), \quad \sigma_{\theta\theta} = \lambda(e_{rr} + e_{\theta\theta}) + 2\mu e_{\theta\theta} - \beta(T + t_1\delta_{2k}\dot{T}) \quad (3)$$

$$\sigma_{r\theta} = 2\mu e_{r\theta} \quad (4)$$

where $\sigma_{rr}, \sigma_{\theta\theta}, \sigma_{r\theta}$ are the stress components, $e_{rr}, e_{\theta\theta}, e_{r\theta}$ are the strain components, T is the temperature change about the equilibrium temperature T_0 , ρ is the mass density, c_v is the specific heat capacity, β is the thermal capacity factor that couples the heat conduction and elastic field equations, K is the thermal conductivity, t_0, t_1 are the two thermal relaxation times, t is the time, λ and μ are Lamé's constants. The comma notation is used for spatial derivatives; the superposed dot represents time differentiation, and δ_{ij} is the Kronecker delta. In addition, $k = 1$ for Lord-Shulman (LS) theory and $k = 2$ for Green-Lindsay (GL) theory. The thermal relaxation times t_0 and t_1 satisfy the inequalities $t_0 \geq t_1 \geq 0$ for GL theory only and we assume that $\rho > 0, T_0 > 0$, and $c_v > 0$. The strain e_{ij} related to the displacements are given by

$$e_{rr} = u_{r,r}, e_{\theta\theta} = r^{-1}(u_r + u_{\theta,\theta}), e_{r\theta} = u_{\theta,r} - r^{-1}(u_\theta - u_{r,\theta}) \quad (5)$$

2.1 Lord-Shulman (LS) thermoelastic model

The Lord-Shulman theory of heat conduction equation is obtained by substituting $k = 1$ in the Eqs. (2) and (3)

$$K(T_{,rr} + r^{-1}T_{,r} + r^{-2}T_{,\theta\theta}) - \rho c_v(\dot{T} + t_0\ddot{T}) = T_0 \left(\frac{\partial}{\partial t} + t_0 \frac{\partial^2}{\partial t^2} \right) \left[\beta(u_{r,r} + r^{-1}(u_{\theta,\theta} + u_r)) \right] \quad (6)$$

and

$$\sigma_{rr} = \lambda(e_{rr} + e_{\theta\theta}) + 2\mu e_{rr} - \beta T, \quad \sigma_{\theta\theta} = \lambda(e_{rr} + e_{\theta\theta}) + 2\mu e_{\theta\theta} - \beta T \quad (7)$$

Substituting Eqs.(3)-(5) and (7) in Eqs.(1) and (6), the displacement equations of motions are obtained as:

$$\begin{aligned}
& (\lambda + 2\mu)(u_{r,rr} + r^{-1}u_{r,r} - r^{-2}u_r) + \mu r^{-2}u_{r,\theta\theta} + r^{-1}(\lambda + \mu)u_{\theta,r\theta} + r^{-2}(\lambda + 3\mu)u_{\theta,\theta} - \beta T_{,r} = \rho \ddot{u}_r \\
& \mu(u_{\theta,rr} + r^{-1}u_{\theta,r} - r^{-2}u_\theta) + r^{-2}(\lambda + 2\mu)u_{\theta,\theta\theta} + r^{-2}(\lambda + 3\mu)u_{r,\theta} + r^{-1}(\lambda + \mu)u_{r,r\theta} - \beta T_{,\theta} = \rho \ddot{u}_\theta \\
& K(T_{,rr} + r^{-1}T_{,r} + r^{-2}T_{,\theta\theta}) - \rho c_v(\dot{T} + t_0\ddot{T}) - T_0\left(\frac{\partial}{\partial t} + t_0\frac{\partial^2}{\partial t^2}\right)\left[\beta(u_{r,r} + r^{-1}(u_{\theta,\theta} + u_r))\right]
\end{aligned} \tag{8}$$

3 SOLUTION OF THE PROBLEM

Eq.(8) is a coupled partial differential equation with two displacements and heat conduction components. To uncouple Eq.(8), we follow the solutions by Mirsky [32] by assuming that the vibration and displacements along the axial direction z is equal to zero, and assuming the solutions of the Eq.(8) in the form

$$\begin{aligned}
u_r(r, \theta, t) &= \sum_{n=0}^{\infty} \varepsilon_n \left[(\phi_{n,r} + r^{-1}\psi_{n,\theta}) + (\bar{\phi}_{n,r} + r^{-1}\bar{\psi}_{n,\theta}) \right] e^{i\alpha t} \\
u_\theta(r, \theta, t) &= \sum_{n=0}^{\infty} \varepsilon_n \left[(r^{-1}\phi_{n,\theta} - \psi_{n,r}) + (r^{-1}\bar{\phi}_{n,\theta} - \bar{\psi}_{n,r}) \right] e^{i\alpha t} \\
T(r, \theta, t) &= (\lambda + 2\mu/\beta a^2) \sum_{n=0}^{\infty} \varepsilon_n (T_n + \bar{T}_n) e^{i\alpha t}
\end{aligned} \tag{9}$$

where $\varepsilon_n = \frac{1}{2}$ for $n = 0$, $\varepsilon_n = 1$ for $n \geq 1$, $i = \sqrt{-1}$, ω is the angular frequency, $\phi_n(r, \theta)$, $\psi_n(r, \theta)$, $T_n(r, \theta)$, $\bar{\phi}_n(r, \theta)$, $\bar{\psi}_n(r, \theta)$ and $\bar{T}_n(r, \theta)$ are the displacement potentials. To facilitate the solution following dimensionless quantities are introduced: $\bar{\lambda} = \frac{\lambda}{\mu}$, $x = \frac{r}{a}$, $\tau_0 = (1 + t_0 i \omega)$, $\bar{K} = K \sqrt{\rho \mu} / \tau_0 \beta^2 a T_0 \Omega$, $\bar{d} = \rho c_v \mu / \beta^2 T_0$, $T_a = t \sqrt{\mu / \rho a}$, $\tau_1 = (1 + t_1 i \omega)$, $c_i^2 = (\lambda + 2\mu) / \rho$, $\Omega^2 = \omega^2 a^2 / c_1^2$, c_1^2 is the phase velocity. Substituting Eq.(9) in Eq.(8), we obtain

$$\left\{ (2 + \lambda) \nabla^2 + \Omega^2 \right\} \phi_n - T_n = 0, \quad \left\{ \nabla^2 \phi_n + (i \bar{K} \nabla^2 + \bar{d}) T_n \right\} = 0 \tag{10}$$

and

$$(\nabla^2 + \Omega^2) \psi_n = 0 \tag{11}$$

where $\nabla^2 = \partial^2 / \partial x^2 + x^{-1} \partial / \partial x + x^{-2} \partial^2 / \partial \theta^2$, Eliminating T_n from the Eq. (10), we obtain

$$(A \nabla^4 + B \nabla^2 + C) \phi_n = 0 \tag{12}$$

where

$$A = i \bar{K}_1 (2 + \bar{\lambda}), B = \left\{ (2 + \lambda) \bar{d} + i \bar{K} \Omega^2 + 1 \right\}, C = \Omega^2 \bar{d} \tag{13}$$

In which A , B and C are arbitrary constants and are used to find the roots of the Eq. (12). The solution of Eq. (12) for the symmetric mode is

$$\phi_n = \sum_{i=1}^2 [A_{in} J_n(\alpha_i \alpha x) + B_{in} Y_n(\alpha_i \alpha x)] \cos n\theta, \quad T_n = \sum_{i=1}^2 a_i [A_{in} J_n(\alpha_i \alpha x) + B_{in} Y_n(\alpha_i \alpha x)] \cos n\theta \quad (14)$$

where J_n is the Bessel function of first kind of order n and Y_n is the Bessel function of second kind of order n , $(\alpha_i a)^2$ are the roots of the equation $A(\alpha a)^4 - B(\alpha a)^2 + C = 0$ and the constant $a_i = \left((2 + \bar{\lambda}) \nabla^2 + \Omega^2 \right), i = 1, 2$.

Solving Eq.(11), we get the solution for the symmetric mode as:

$$\psi_n = [A_{3n} J_n(\alpha_3 \alpha x) + B_{3n} Y_n(\alpha_3 \alpha x)] \sin n\theta \quad (15)$$

The solutions for the antisymmetric mode $\bar{\phi}_n, \bar{T}_n$ and $\bar{\psi}_n$ are obtained from Eqs. (14) and (15) by replacing $\sin n\theta$ by $\cos n\theta$ and $\cos n\theta$ by $\sin n\theta$. If $(\alpha_i a)^2 < 0$ ($i = 1, 2, 3$), then the Bessel functions J_n and Y_n are to be replaced by the modified Bessel function I_n and K_n respectively. The integration constants A_{in}, B_{in} ($i = 1, 2, 3$) are to be determined from the boundary conditions.

4 BOUNDARY CONDITIONS AND FREQUENCY EQUATIONS

In this problem, the free vibration of polygonal (triangle, square, pentagon and hexagon) plate of inner and outer cross sections is considered. Since the boundary of the polygonal cross-sectional plate is irregular in shape, it is difficult to satisfy the boundary conditions along the outer and inner surface of the plate directly. Hence, from context of Nagaya [1,2,3,4,5], the Fourier expansion collocation method is applied. Thus, the boundary conditions along the outer boundary of the plate is obtained as:

$$(\sigma_{xx})_i = (\sigma_{xy})_i = (T)_i = 0 \quad (16)$$

and for the inner boundary, the boundary conditions are

$$(\sigma'_{xx})_i = (\sigma'_{xy})_i = (T')_i = 0 \quad (17)$$

where x is the coordinate normal to the boundary and y is the coordinate tangential to the boundary, $\sigma_{xx}, \sigma'_{xx}$ are the normal stresses, $\sigma_{xy}, \sigma'_{xy}$ are the shearing stresses, T, T' are the thermal fields and $()_i$ is the value at the i -th segment of the outer and inner boundary respectively. Since the angle γ_i between the reference axis and the normal to the i -th straight line boundary has a constant value in the segment as shown in Fig. 2, we can obtain the transformed equations of the normal stress σ'_{xx} and shearing stress σ'_{xy} for the i -th segment of the boundary are expressed as Nagaya [4] is

$$\begin{aligned} \sigma'_{xx} &= \lambda (u_{r,r} + r^{-1} (u_r + u_{\theta,\theta})) + 2\mu \{ u_{r,r} \cos^2(\theta - \gamma_i) + r^{-1} (u_r + u_{\theta,\theta}) \sin^2(\theta - \gamma_i) \\ &\quad + 0.5 (r^{-1} (u_{\theta} - u_{r,\theta}) - u_{\theta,r}) \sin 2(\theta - \gamma_i) \} - \beta T \\ \sigma'_{xy} &= \mu (u_{r,r} - r^{-1} (u_{\theta,\theta} + u_r) \sin 2(\theta - \gamma_i) + (r^{-1} (u_{r,\theta} - u_{\theta}) + u_{\theta,r}) \sin 2(\theta - \gamma_i)) \end{aligned} \quad (18)$$

Substituting Eqs.(14), (15) in Eqs.(16) and (17), and performing Fourier series expansion to the boundary, the boundary condition along the inner and outer surfaces are expanded in the form of double Fourier series. When the plate is symmetric about more than one axis, the boundary conditions in the case of symmetric mode can be written in the form of a matrix as given below:

$$\begin{pmatrix}
 E_{00}^1 & E_{00}^2 & E_{00}^3 & E_{00}^4 & E_{01}^1 & \dots & E_{0N}^1 & E_{01}^2 & \dots & E_{0N}^2 & E_{01}^3 & \dots & E_{0N}^3 & E_{01}^4 & \dots & E_{0N}^4 & E_{01}^5 & \dots & E_{0N}^5 & E_{01}^6 & \dots & E_{0N}^6 \\
 \vdots & \vdots & \vdots & \vdots & \vdots & \dots & \vdots & \vdots & \dots & \vdots & \vdots & \dots & \vdots & \vdots & \dots & \vdots & \vdots & \dots & \vdots & \vdots & \dots & \vdots \\
 E_{N0}^1 & E_{N0}^2 & E_{N0}^3 & E_{N0}^4 & E_{N1}^1 & \dots & E_{NN}^1 & E_{N1}^2 & \dots & E_{NN}^2 & E_{N1}^3 & \dots & E_{NN}^3 & E_{N1}^4 & \dots & E_{NN}^4 & E_{N1}^5 & \dots & E_{NN}^5 & E_{N1}^6 & \dots & E_{NN}^6 \\
 F_{10}^1 & F_{10}^2 & F_{10}^3 & F_{10}^4 & F_{11}^1 & \dots & F_{1N}^1 & F_{11}^2 & \dots & F_{1N}^2 & F_{11}^3 & \dots & F_{1N}^3 & F_{11}^4 & \dots & F_{1N}^4 & F_{11}^5 & \dots & F_{1N}^5 & F_{11}^6 & \dots & F_{1N}^6 \\
 \vdots & \vdots & \vdots & \vdots & \vdots & \dots & \vdots & \vdots & \dots & \vdots & \vdots & \dots & \vdots & \vdots & \dots & \vdots & \vdots & \dots & \vdots & \vdots & \dots & \vdots \\
 F_{N0}^1 & F_{N0}^2 & F_{N0}^3 & F_{N0}^4 & F_{N1}^1 & \dots & F_{NN}^1 & F_{N1}^2 & \dots & F_{NN}^2 & F_{N1}^3 & \dots & F_{NN}^3 & F_{N1}^4 & \dots & F_{NN}^4 & F_{N1}^5 & \dots & F_{NN}^5 & F_{N1}^6 & \dots & F_{NN}^6 \\
 G_{00}^1 & G_{00}^2 & G_{00}^3 & G_{00}^4 & G_{01}^1 & \dots & G_{0N}^1 & G_{01}^2 & \dots & G_{0N}^2 & G_{01}^3 & \dots & G_{0N}^3 & G_{01}^4 & \dots & G_{0N}^4 & G_{01}^5 & \dots & G_{0N}^5 & G_{01}^6 & \dots & G_{0N}^6 \\
 \vdots & \vdots & \vdots & \vdots & \vdots & \dots & \vdots & \vdots & \dots & \vdots & \vdots & \dots & \vdots & \vdots & \dots & \vdots & \vdots & \dots & \vdots & \vdots & \dots & \vdots \\
 G_{N0}^1 & G_{N0}^2 & G_{N0}^3 & G_{N0}^4 & G_{N1}^1 & \dots & G_{NN}^1 & G_{N1}^2 & \dots & G_{NN}^2 & G_{N1}^3 & \dots & G_{NN}^3 & G_{N1}^4 & \dots & G_{NN}^4 & G_{N1}^5 & \dots & G_{NN}^5 & G_{N1}^6 & \dots & G_{NN}^6 \\
 E_{00}^1 & E_{00}^2 & E_{00}^3 & E_{00}^4 & E_{10}^1 & \dots & E_{0N}^1 & E_{10}^2 & \dots & E_{0N}^2 & E_{10}^3 & \dots & E_{0N}^3 & E_{10}^4 & \dots & E_{0N}^4 & E_{10}^5 & \dots & E_{0N}^5 & E_{10}^6 & \dots & E_{0N}^6 \\
 \vdots & \vdots & \vdots & \vdots & \vdots & \dots & \vdots & \vdots & \dots & \vdots & \vdots & \dots & \vdots & \vdots & \dots & \vdots & \vdots & \dots & \vdots & \vdots & \dots & \vdots \\
 E_{N0}^1 & E_{N0}^2 & E_{N0}^3 & E_{N0}^4 & E_{N1}^1 & \dots & E_{NN}^1 & E_{N1}^2 & \dots & E_{NN}^2 & E_{N1}^3 & \dots & E_{NN}^3 & E_{N1}^4 & \dots & E_{NN}^4 & E_{N1}^5 & \dots & E_{NN}^5 & E_{N1}^6 & \dots & E_{NN}^6 \\
 F_{10}^1 & F_{10}^2 & F_{10}^3 & F_{10}^4 & F_{11}^1 & \dots & F_{1N}^1 & F_{11}^2 & \dots & F_{1N}^2 & F_{11}^3 & \dots & F_{1N}^3 & F_{11}^4 & \dots & F_{1N}^4 & F_{11}^5 & \dots & F_{1N}^5 & F_{11}^6 & \dots & F_{1N}^6 \\
 \vdots & \vdots & \vdots & \vdots & \vdots & \dots & \vdots & \vdots & \dots & \vdots & \vdots & \dots & \vdots & \vdots & \dots & \vdots & \vdots & \dots & \vdots & \vdots & \dots & \vdots \\
 F_{N0}^1 & F_{N0}^2 & F_{N0}^3 & F_{N0}^4 & F_{N1}^1 & \dots & F_{NN}^1 & F_{N1}^2 & \dots & F_{NN}^2 & F_{N1}^3 & \dots & F_{NN}^3 & F_{N1}^4 & \dots & F_{NN}^4 & F_{N1}^5 & \dots & F_{NN}^5 & F_{N1}^6 & \dots & F_{NN}^6 \\
 G_{00}^1 & G_{00}^2 & G_{00}^3 & G_{00}^4 & G_{01}^1 & \dots & G_{0N}^1 & G_{01}^2 & \dots & G_{0N}^2 & G_{01}^3 & \dots & G_{0N}^3 & G_{01}^4 & \dots & G_{0N}^4 & G_{01}^5 & \dots & G_{0N}^5 & G_{01}^6 & \dots & G_{0N}^6 \\
 \vdots & \vdots & \vdots & \vdots & \vdots & \dots & \vdots & \vdots & \dots & \vdots & \vdots & \dots & \vdots & \vdots & \dots & \vdots & \vdots & \dots & \vdots & \vdots & \dots & \vdots \\
 G_{N0}^1 & G_{N0}^2 & G_{N0}^3 & G_{N0}^4 & G_{N1}^1 & \dots & G_{NN}^1 & G_{N1}^2 & \dots & G_{NN}^2 & G_{N1}^3 & \dots & G_{NN}^3 & G_{N1}^4 & \dots & G_{NN}^4 & G_{N1}^5 & \dots & G_{NN}^5 & G_{N1}^6 & \dots & G_{NN}^6
 \end{pmatrix} = 0 \quad (19)$$

In which

$$\begin{aligned}
 E_{mn}^j &= 2\varepsilon_n/\pi \int_{\theta_{i-1}}^{\theta_i} \int_{r_i}^{\hat{r}} e_n^j R_i, \theta \cos m\theta d\theta, F_{mn}^j = 2\varepsilon_n/\pi \int_{\theta_{i-1}}^{\theta_i} \int_{r_i}^{\hat{r}} f_n^j R_i, \theta \sin m\theta d\theta \\
 G_{mn}^j &= 2\varepsilon_n/\pi \int_{\theta_{i-1}}^{\theta_i} \int_{r_i}^{\hat{r}} g_n^j R_i, \theta \cos m\theta d\theta, E_{mn}^j = 2\varepsilon_n/\pi \int_{\theta_{i-1}}^{\theta_i} \int_{r_i}^{\hat{r}} e_n^j R_i, \theta \cos m\theta d\theta \\
 F_{mn}^j &= 2\varepsilon_n/\pi \int_{\theta_{i-1}}^{\theta_i} \int_{r_i}^{\hat{r}} f_n^j R_i, \theta \sin m\theta d\theta, G_{mn}^j = 2\varepsilon_n/\pi \int_{\theta_{i-1}}^{\theta_i} \int_{r_i}^{\hat{r}} g_n^j R_i, \theta \cos m\theta d\theta
 \end{aligned} \quad (20)$$

where $j = 1, 2, 3, 4, 5$ and 6 , I is the number of segments, R_i is the coordinate \hat{r} at the inner boundary, R_i is the coordinate r at the outer boundary and N is the number of truncation of the Fourier series. The coefficients $e_n^j \sim g_n^j$ are given in Appendix A.

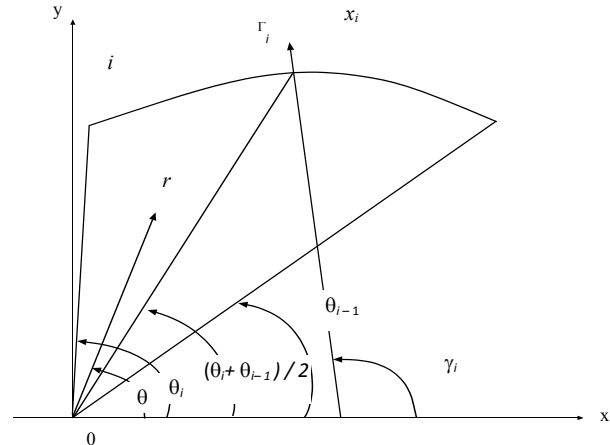


Fig.2 Geometry of a straight line segment.

4.1 Boundary conditions and frequency equation for clamped edge boundary

The boundary conditions for rigidly fixed boundary is obtained by assuming that the displacements along the radial direction u_r , along the circumferential direction u_θ and the thermal field T is equal to zero, thus we get the boundary condition for the outer surface as:

$$(u_r)_i = (u_\theta)_i = (T)_i = 0$$

and the boundary condition for the inner surface of the plate as:

$$(u_r')_i = (u_\theta')_i = (T')_i = 0 \quad (21)$$

Using Eq. (9) in Eq. (21), we can obtain the frequency equations for rigidly fixed boundary in the following form; $|b_{ij}| = 0, (i, j = 1, 2, 3, 4, 5, 6)$. Where

$$\begin{aligned} b_{1i} &= \{nJ_n(\alpha_i ax) - (\alpha_i ax)J_{n+1}(\alpha_i ax)\}, i = 1, 2, & b_{13} &= nJ_n(\alpha_3 ax) \\ b_{2i} &= nJ_n(\alpha_i ax), i = 1, 2, & b_{23} &= \{nJ_n(\alpha_3 ax) - (\alpha_3 ax)J_{n+1}(\alpha_3 ax)\} \\ b_{3i} &= d_i J_n(\alpha_i ax), i = 1, 2, & b_{33} &= 0 \\ b_{4i} &= \{nJ_n(\alpha_i bx) - (\alpha_i bx)J_{n+1}(\alpha_i bx)\}, i = 1, 2, & b_{43} &= nJ_n(\alpha_3 bx) \\ b_{5i} &= nJ_n(\alpha_i bx), i = 1, 2, & b_{53} &= \{nJ_n(\alpha_3 bx) - (\alpha_3 bx)J_{n+1}(\alpha_3 bx)\} \\ b_{6i} &= d_i J_n(\alpha_i ax), i = 1, 2, & b_{63} &= 0 \end{aligned} \quad (22)$$

The remaining terms $b_{ij}, b_{2j}, b_{3j}, b_{4j}, b_{5j}, b_{6j}, (j = 4, 5, 6)$ are obtained by replacing J_n and J_{n+1} with Y_n and Y_{n+1} respectively, and the constant $d_i = \left[\Omega^2 - (\alpha_i a)^2 (2 + \bar{\lambda}) \right]$.

5 NUMERICAL RESULTS AND DISCUSSION

The numerical analysis of the frequency equation is carried out for generalized thermoelastic doubly connected polygonal (square, triangle, pentagon and hexagon) plates, and the dimensions of each plate used in the numerical calculation are shown in Fig. 2. The computation of Fourier coefficients given in Eq.(20) is carried out using the five point Gaussian quadrature. The material properties of copper at $42^\circ K$ are taken from Erbay and Suhubi [11] as Poisson ratio $\nu = 0.3$ density $\rho = 8.96 \times 10^3 \text{ kg/m}^3$ the Young's modulus $E = 2.139 \times 10^{11} \text{ N/m}^2$, $\lambda = 8.20 \times 10^{11} \text{ kg/ms}^2$, $\mu = 4.20 \times 10^{10} \text{ kg/ms}^2$, $c_v = 9.1 \times 10^{-2} \text{ m}^2/\text{ks}^2$ and $K = 113 \times 10^{-2} \text{ kgm/ks}^2$, and the thermal relaxation time considered from Sharma and Sharma [12] as $t_0 = 0.75 \times 10^{-13} \text{ sec}$. The geometric relations for the polygonal cross-sections given by Nagaya [4]

$$R_i/b = [\cos(\theta - \gamma_i)]^{-1} \quad (23)$$

where b is the apothem. In the numerical calculation, the angle θ is taken as an independent variable and the coordinate R_i and R_i are at the i -th segment of the boundary is expressed in terms of θ . Substituting R_i, R_i and the angle γ_i , between the reference axis and the normal to the i th boundary line, the integrations of the Fourier

coefficients $e_n^i, f_n^i, g_n^i, \bar{e}_n^i, \bar{f}_n^i$, and \bar{g}_n^i can be expressed in terms of the angle θ . Using these coefficients in to the Eq.(20), the frequencies are obtained for generalized thermoelastic polygonal plate.

5.1 Longitudinal mode of polygonal plates

In longitudinal mode of square and hexagonal cross-section, the cross-section vibrates along the axis of the plate, so that the vibration displacements in the cross-sections are symmetrical about both the major and the minor axes. Hence the frequency equations are obtained by choosing both the terms of m and n as 0,2,4,6,... in Eq. (19) for the numerical calculations. In the case of triangle and pentagonal shaped plate, the vibration and displacements are symmetrical about the major axis alone, hence the frequency equations are obtained from Eq. (19) by choosing m and n as 0,1,2,3,... Since the boundary of the plate namely, triangle, square, pentagon and hexagon are irregular, it is difficult to satisfy the boundary conditions along the curved surface, and hence Fourier expansion collocation method is applied. That is the curved surface, in the range $\theta = 0$ and $\theta = \pi$ is divided into 20 segments, such that the distance between any two segments is negligible and the integrations is performed for each segment numerically by using the Gauss five point formula. The non-dimensional frequencies are computed for $0 < \Omega \leq 1.0$, using the secant method (applicable for the complex roots, (Antia [33])).

5.2 Flexural mode of polygonal plates

In flexural mode of square and hexagonal cross-section, the vibration and displacements are antisymmetrical about the major axis and symmetrical about the minor axis. Hence the frequency equation is obtained from Eq. (19) by changing $\cos n\theta$ by $\sin n\theta$ and $\sin n\theta$ by $\cos n\theta$ and choosing $n, m = 1, 3, 5, 7, \dots$. In the case of triangle and pentagonal plate, the vibration and displacements are antisymmetrical about the minor axis, hence the frequency equations is obtained by choosing $n, m = 1, 2, 3, \dots$. The geometric relation for the polygonal plate is given in Eq. (23), which is used for the numerical calculation. The notations used in the figures namely ICOF and IFOC denote the Inner Clamped and Outer Free edges and Inner Free and Outer Clamped edges, respectively.

5.3 Dispersion analysis

The Variation of non-dimensional wave number versus non-dimensional frequency of longitudinal modes of polygonal cross-sectional plate is discussed with different boundary conditions and aspect ratio in Figs. 3-6. From Figs. 3 and 4, the dispersion of the non-dimensional wave number is steady and increasing in triangular and square cross sectional plates for the longitudinal modes. This behavior is observed oscillating in Figs. 5 and 6 for the flexural antisymmetric modes of pentagonal and hexagonal cross sections with increasing aspect ratio. The effect of wave number of the inner boundary when it is free or simply supported is large compared with that of inner clamped edge boundary conditions.

Graphs are drawn for ICOF and IFOC edge boundary conditions for the velocity versus dimensionless frequency for longitudinal modes of triangular and square plates respectively and are shown in the Fig.7 and Fig.8. From the Figs.7 and 8, it is observed that, the velocity increases with respect to its non dimensional frequency, also it is noted that the velocity for IFOC surface have higher in magnitude than the velocity of ICOF edge boundary conditions. The wave velocity is minimum in the lower range of frequency and increase for higher modes of frequency, and the cross over points in the trend line indicates, the transfer of heat energy between the modes of vibrations. The transfer of heat energy in the distribution of velocity is higher in the lower modes of frequency and become steady in the higher modes of frequency.

A comparison is made between wave velocity and non dimensional frequency with ICOF and IFOC edge boundary conditions of longitudinal and flexural antisymmetric modes of pentagonal and hexagonal cross sections in Fig. 9 and Fig. 10. From the Figs. 9 and 10, it is observed that the velocity is higher for a ICOF plate as comparing with the other boundary condition IFOC. From the figures, it is observed that the increasing trend both in frequency and velocity with little deviations in the dispersion characteristics is an indication of up gradation of strength of material. The crossover points denote the transfer of heat energy between the modes of vibrations.

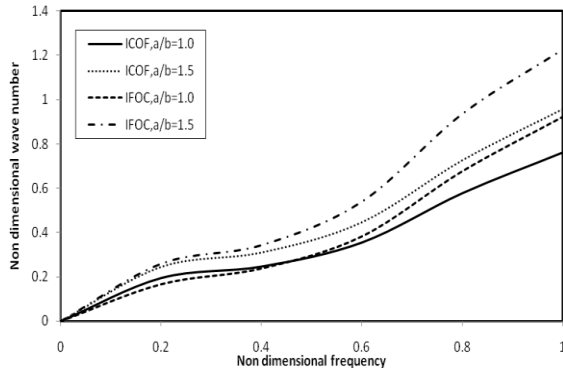


Fig.3
Variation of non-dimensional wave number versus non-dimensional frequency of longitudinal modes of triangular cross-sectional plate.

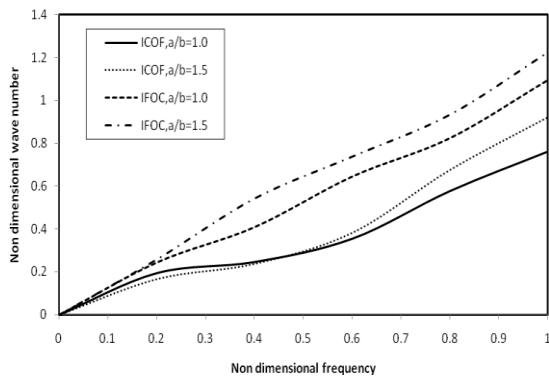


Fig.4
Variation of non-dimensional wave number versus non-dimensional frequency of longitudinal modes of square cross-sectional plate.

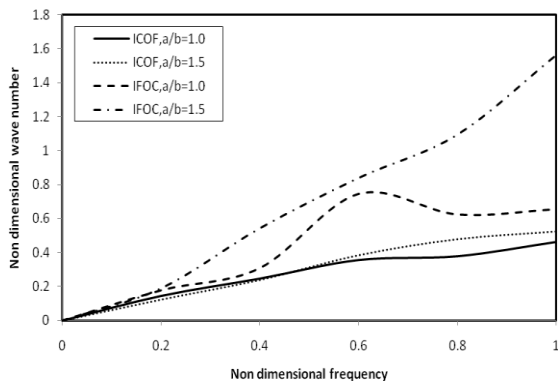


Fig.5
Variation of non-dimensional wave number versus non-dimensional frequency of flexural anti symmetric modes for pentagonal cross-sectional plate.

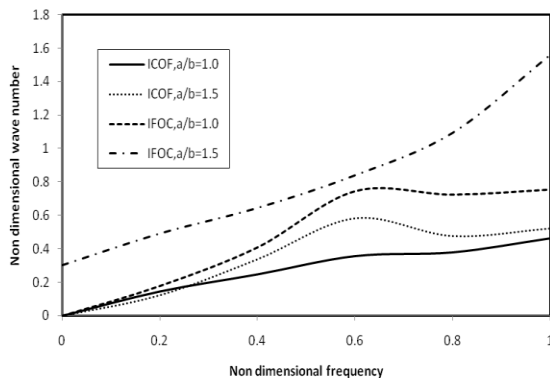


Fig.6
Variation of non-dimensional wave number versus non-dimensional frequency of flexural anti symmetric modes for hexagonal cross-sectional plate.

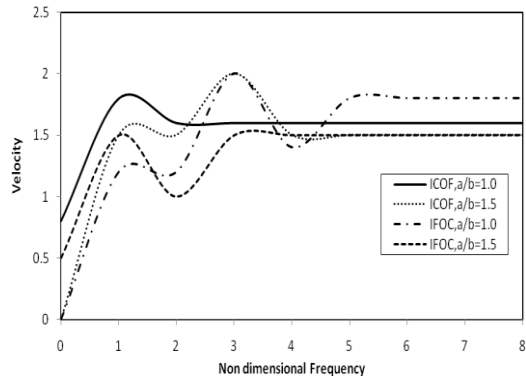


Fig.7
Variation of velocity versus non-dimensional frequency of longitudinal modes for triangular cross-sectional plate.

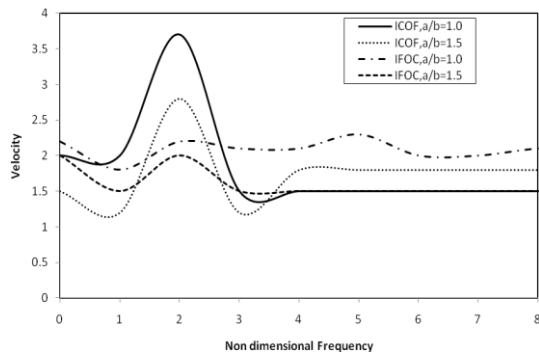


Fig.8
Variation of velocity versus non-dimensional frequency of longitudinal modes for square cross-sectional plate.

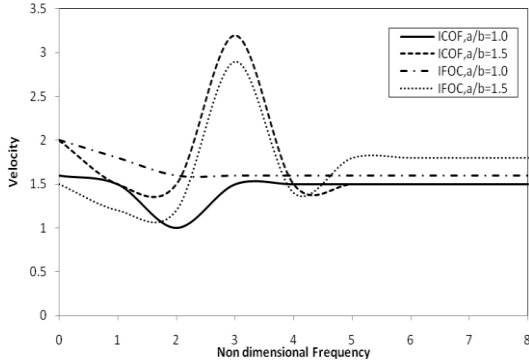


Fig.9
Variation of velocity versus non-dimensional frequency of longitudinal modes for pentagonal cross-sectional plate.

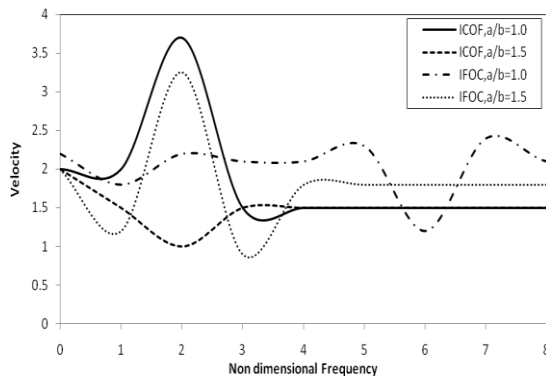


Fig.10
Variation of velocity versus non-dimensional frequency of longitudinal modes for hexagonal cross-sectional plate.

APPENDIX A

The expressions $e_n^i \sim g_n^i$ used in Eq. (20) are given as follows:

$$e_n^i = 2\{n(n-1)J_n(\alpha_i ax) + (\alpha_i ax)J_{n+1}(\alpha_i ax)\} \cos 2(\theta - \gamma_i) \cos n\theta - x^2 \left\{ (\alpha_i a)^2 + [\bar{\lambda} + 2 \cos^2(\theta - \gamma_i)] + a_i \right\} J_n(\alpha_i ax) \cos n\theta + 2n \{ (n-1)J_n(\alpha_i ax) - (\alpha_i ax)J_{n+1}(\alpha_i ax) \} \sin n\theta \sin 2(\theta - \gamma_i), \quad i = 1, 2 \quad (\text{A.1})$$

$$e_n^3 = 2\{n(n-1)J_n(\alpha_3 ax) - (\alpha_3 ax)J_{n+1}(\alpha_3 ax)\} \cos n\theta \cos 2(\theta - \gamma_i) + 2\{[n(n-1) - (\alpha_3 ax)^2]J_n(\alpha_3 ax) + (\alpha_3 ax)J_{n+1}(\alpha_3 ax)\} \sin n\theta \sin 2(\theta - \gamma_i) \quad (\text{A.2})$$

$$e_n^4 = 2\{n(n-1)Y_n(\alpha_4 ax) - (\alpha_4 ax)Y_{n+1}(\alpha_4 ax)\} \cos n\theta \cos 2(\theta - \gamma_i) + 2\{[n(n-1) - (\alpha_4 ax)^2]Y_n(\alpha_4 ax) + (\alpha_4 ax)Y_{n+1}(\alpha_4 ax)\} \sin n\theta \sin 2(\theta - \gamma_i) \quad (\text{A.3})$$

$$e_n^i = 2\{n(n-1)Y_n(\alpha_i ax) + (\alpha_i ax)Y_{n+1}(\alpha_i ax)\} \cos 2(\theta - \gamma_i) \cos n\theta - x^2 \left\{ (\alpha_i a)^2 + [\bar{\lambda} + 2 \cos^2(\theta - \gamma_i)] + a_i \right\} Y_n(\alpha_i ax) \cos n\theta + 2n \{ (n-1)Y_n(\alpha_i ax) - (\alpha_i ax)Y_{n+1}(\alpha_i ax) \} \sin n\theta \sin 2(\theta - \gamma_i), \quad i = 5, 6 \quad (\text{A.4})$$

$$f_n^i = 2\{[n(n-1) - (\alpha_i ax)^2]J_n(\alpha_i ax) + (\alpha_i ax)J_{n+1}(\alpha_i ax)\} \cos n\theta \sin 2(\theta - \gamma_i) + 2n \{ (\alpha_i ax)J_{n+1}(\alpha_i ax) - (n-1)J_n(\alpha_i ax) \} \sin n\theta \cos 2(\theta - \gamma_i), i = 1, 2 \quad (\text{A.5})$$

$$f_n^3 = 2n \{ (n-1)J_n(\alpha_3 ax) - (\alpha_3 ax)J_{n+1}(\alpha_3 ax) \} \cos n\theta \sin 2(\theta - \gamma_i) - \{ 2(\alpha_3 ax)J_{n+1}(\alpha_3 ax) - [(\alpha_3 ax)^2 - 2n(n-1)]J_n(\alpha_3 ax) \} \sin n\theta \cos 2(\theta - \gamma_i) \quad (\text{A.6})$$

$$f_n^4 = 2n \{ (n-1)Y_n(\alpha_4 ax) - (\alpha_4 ax)Y_{n+1}(\alpha_4 ax) \} \cos n\theta \sin 2(\theta - \gamma_i) - \{ 2(\alpha_4 ax)Y_{n+1}(\alpha_4 ax) - [(\alpha_4 ax)^2 - 2n(n-1)]Y_n(\alpha_4 ax) \} \sin n\theta \cos 2(\theta - \gamma_i) \quad (\text{A.7})$$

$$f_n^i = 2\{[n(n-1) - (\alpha_i ax)^2]Y_n(\alpha_i ax) + (\alpha_i ax)Y_{n+1}(\alpha_i ax)\} \cos n\theta \sin 2(\theta - \gamma_i) + 2n \{ (\alpha_i ax)Y_{n+1}(\alpha_i ax) - (n-1)Y_n(\alpha_i ax) \} \sin n\theta \cos 2(\theta - \gamma_i), i = 5, 6 \quad (\text{A.8})$$

$$k_n^i = d_i \left\{ n \cos(\overline{n-1}\theta + \gamma_i) J_n(\alpha_i ax) - (\alpha_i ax) J_{n+1}(\alpha_i ax) \cos(\theta - \gamma_i) \cos n\theta \right\}, i = 1, 2 \quad (\text{A.9})$$

$$k_n^3 = 0.0, k_n^4 = 0.0 \quad (\text{A.10})$$

$$k_n^i = d_i \left\{ n \cos(\overline{n-1}\theta + \gamma_i) Y_n(\alpha_i ax) - (\alpha_i ax) Y_{n+1}(\alpha_i ax) \cos(\theta - \gamma_i) \cos n\theta \right\}, i = 5, 6 \quad (\text{A.11})$$

The expressions $e_n^{-i} \sim g_n^{-i}$ is obtained by replacing $\cos n\theta$ by $\sin n\theta$ and $\sin n\theta$ by $\cos n\theta$ by the Eqs. (A.1) - (A.11).

6 CONCLUSIONS

Free vibration analysis of generalized thermoelastic polygonal shaped plate of inner and outer cross section is studied using the Fourier expansion collocation method. The equations of motion based on two-dimensional theory of elasticity are applied under the plane strain assumption of generalized thermoelastic plate of polygonal shape composed of homogeneous isotropic material. The frequency equations are obtained by satisfying the boundary conditions along the inner and outer surface of the polygonal plate. The numerical calculations are carried out for triangular, square, pentagonal and hexagonal shaped plates. The dispersion curves are drawn for longitudinal and flexural antisymmetric modes of polygonal plates. The polygonal plates, as structural elements, are widely used in construction of oil pipes, submarine and flight structures to ensure the strength and reliability, acted upon by nonuniform loads.

REFERENCES

- [1] Nagaya K., 1981, Simplified method for solving problems of plates of doubly connected arbitrary shape, Part I: Derivation of the frequency equation, *Journal of Sound and Vibration* **74**(4): 543-551.
- [2] Nagaya K., 1981, Simplified method for solving problems of plates of doubly connected arbitrary shape, Part II: Applications and experiments, *Journal of Sound and Vibration* **74**(4): 553-564.
- [3] Nagaya K., 1981, Dispersion of elastic waves in bar with polygonal cross-section, *Journal of Acoustical Society of America* **70**(3): 763-770.
- [4] Nagaya K., 1983, Vibration of a thick walled pipe or ring of arbitrary shape in its Plane, *Journal of Applied Mechanics* **50**: 757-764.
- [5] Nagaya K., 1983, Vibration of a thick polygonal ring in its plane, *Journal of Acoustical Society of America* **74**(5): 1441-1447.
- [6] Lord H.W., Shulman Y., 1967, A generalized dynamical theory of thermo elasticity, *Journal of Mechanics of Physics of Solids* **5**: 299-309.
- [7] Dhaliwal R.S., Sherief H.H., 1980, Generalized thermo elasticity for anisotropic media, *Quarterly Applied Mathematics* **8**(1): 1-8.
- [8] Green A.E., Laws N., 1972, On the entropy production inequality, *Archive of Rational Mechanical Analysis* **45**: 47-53.
- [9] Green A.E., Lindsay K.A., 1972, Thermo elasticity, *Journal of Elasticity* **2**: 1-7.
- [10] Suhubi E.S., 1964, Longitudinal vibrations of a circular cylindrical coupled with a thermal field, *Journal of Mechanics of Physics of Solids* **12**: 69-75.
- [11] Erbay E.S., Suhubi E.S., 1986, Longitudinal wave propagation of thermoelastic cylinder, *Journal of Thermal Stresses* **9**: 279-295.
- [12] Sharma J.N., Sharma P.K., 2002, Free vibration analysis of homogeneous transversely isotropic thermoelastic cylindrical panel, *Journal of Thermal Stresses* **25**: 169-182.
- [13] Sharma J.N., Kumar R., 2004, Asymptotic of wave motion in transversely isotropic plates, *Journal of Sound and Vibration* **274**: 747-759.
- [14] Ashida F., Tauchert T.R., 2001, A general plane-stress solution in cylindrical coordinates for a piezoelectric plate, *International Journal of Solids and Structures* **30**: 4969-4985.
- [15] Ashida F., 2003, Thermally-induced wave propagation in piezoelectric plate, *Acta Mechanica* **161**: 1-16.
- [16] Tso Y.K., Hansen C.H., 1995, Wave propagation through cylinder/plate junctions, *Journal of Sound and Vibration* **186**(3): 447-461.
- [17] Heyliger P.R., Ramirez G., 2000, Free vibration of Laminated circular piezoelectric plates and disc, *Journal of Sound and Vibration* **229**(4): 935-956.
- [18] Gaikward M.K., Deshmukh K.C., 2005, Thermal deflection of an inverse thermoelastic problem in a thin isotropic circular plate, *Journal of Applied Mathematical Modelling* **29**: 797-804.
- [19] Varma K.L., 2002, On the propagation of waves in layered anisotropic media in generalized thermo elasticity, *International Journal of Engineering Sciences* **40**: 2077-2096.
- [20] Ponnusamy P., 2007, Wave propagation in a generalized thermoelastic solid cylinder of arbitrary cross-section, *International Journal of Solids and Structures* **44**: 5336-5348.
- [21] Ponnusamy P., 2013, Wave propagation in a piezoelectric solid bar of circular cross-section immersed in fluid, *International Journal of Pressure Vessels and Piping* **105**: 12-18.
- [22] Jiangong Y., Bin W., Cunfu H., 2010, Circumferential thermoelastic waves in orthotropic cylindrical curved plates without energy dissipation, *Ultrasonics* **53**(3):416-423.
- [23] Jiangong Y., Tonglong X., 2010, Generalized thermoelastic waves in spherical curved plates without energy dissipation, *Acta Mechanica* **212**: 39-50.

- [24] Jiangong Y., Xiaoming Zh., Tonglong X., 2010, Generalized thermoelastic waves in functionally graded plates without energy dissipation, *Composite Structures* **93**(1): 32-39.
- [25] Kumar R. , Chawla V., Abbas I.A., 2012, Effect of viscosity on wave propagation in anisotropic thermoelastic medium with three-phase-lag model, *Theoretical and Applied Mechanics* **39**(4): 313-341.
- [26] Kumar R., Abbas I. A., 2014, Response of thermal source in initially stressed generalized thermoelastic half-space with voids, *Journal of Computational and Theoretical Nanoscience* **11**: 1-8.
- [27] Kumar R., Abbas I. A., Marin M., 2015, Analytical numerical solution of thermoelastic interactions in a semi-infinite medium with one relaxation time, *Journal of Computational and Theoretical Nanoscience* **12**: 1-5.
- [28] Ponnusamy P., Selvamani R., 2012, Dispersion analysis of generalized magneto-thermoelastic waves in a transversely isotropic cylindrical panel, *Journal of Thermal Stresses* **35**: 1119-1142.
- [29] Ponnusamy P., Selvamani R., 2013, Wave propagation in magneto thermo elastic cylindrical panel, *European Journal of Mechanics-A solids* **39**: 76-85.
- [30] Selvamani R., Ponnusamy P., 2013, Wave propagation in a generalized thermo elastic plate immersed in fluid, *Structural Engineering and Mechanics* **46**(6): 827-842.
- [31] Selvamani R., Ponnusamy P., 2014, Dynamic response of a solid bar of cardioid cross-sections immersed in an inviscid fluid, *Applied Mathematics and Information Sciences* **8**(6): 2909-2919.
- [32] Mirsky I., 1964, Wave propagation in a transversely isotropic circular cylinders, Part I: Theory, Part II: Numerical results, *Journal of Acoustical Society of America* **37**(6): 1016-1026.
- [33] Antia H.M., 2002, *Numerical Methods for Scientists and Engineers*, Hindustan Book Agency, New Delhi.